Numerical Tests of the Shear Transformation Zone Theory for Dense Granular Flows

Gregg Lois[(1)], Anaël Lemaître[(1,2)], and Jean M. Carlson[(1)]
[(1)] *Department of physics, University of California, Santa Barbara, California 93106, U.S.A. and*
[(2)] *L.M.D.H. - Universite Paris VI, UMR 7603,*
4 place Jussieu - case 86, 75005 Paris - France
(Dated: September 30, 2004)

We test constitutive equations for dense granular materials proposed in [1] on the basis of the Shear Transformation Zone (STZ) theory [2, 3] of plasticity. In this process we first introduce an invariance in Newton's equations, explain how it leads to Bagnold's scaling, and discuss how it relates to the dynamics of granular temperature. Next we implement numerical simulations of granular materials in two different geometries–simple shear and a flow down an incline–and show that measurements can be extrapolated from one geometry to the other. Then we observe non-affine rearrangements of clusters of grains in response to shear strain and show that fundamental observations in [2, 3], which served as a basis for STZ theory, can be reproduced in granular materials. Finally we present constitutive equations for granular materials, based on the dynamics of granular temperature and STZ theory, and show that they match remarkably well with our numerical data from both geometries.

Prediction of natural phenomena–landslides, earthquakes, dunes–and control of industrial processes–transport of granulates, storage in hoppers– call for a deeper understanding of the mechanics of granular materials. Historically reserved to the engineering community [4–7], granular materials recently emerged as a new frontier of study for physicists [8–12]: a state of matter which is hardly classifiable according to the traditional ternary–solid, liquid or gas– and requires us to rethink the foundations of statistical physics and thermodynamics [13?].

No wonder the elaboration of physically inspired constitutive equations for granular materials is currently facing a body of controversial issues regarding its most fundamental aspects. Common points of contention include: (i) the relevant features of the grain-grain interaction– *e.g.* Hertzian versus hard-sphere repulsion– [12, 14? , 15] (ii) the domain of applicability of kinetic theories(!!Goldhircsh, Azanza Chevois), (iii) the identification of thermodynamic "phases" of granular materials, and their resemblance with thermalized systems [9, 16, 17] (iv) the interpretation of chain forces [18–22] and plausible need to formulate "non-local" constitutive equations, [?] and (v) the observation and micromechanical origin of Bagnold scaling in dense flows. [23–26, 28]

The first theories of granular materials were motivated primarily by the need to predict the creep motion of soils and their stability. Inspired from continuum theories of plasticity, these approaches were naturally restricted to quasi-static deformation and incipient failure. [4–7, 29–31]. In physics, most progress came in dilute granular materials with the development of kinetic theory: modifications of Boltzmann's equation to accommodate the existence of inelastic collisions provides estimates of the rate of energy dissipation and transport coefficients by means of collision integrals [32–44], the accepted results being consistent with rule of thumb estimates [45, 46].

Kinetic theory is based on the implicit assumption that interactions between grains occur during instantaneous binary collisions. However, it became apparent that this condition is verified by very few "rapid" flows outside the laboratory. In dense granular flows, multicontact interaction result from inelastic collapse [47, 48] and contribute to the emergence of a "static" or "frictional" contribution to the stress [49, 50].

The breakdown of kinetic theory in dense flows has now been characterized in several numerical and experimental [49–56] studies, and calls for further exploration of elementary mechanisms of jamming. Uncertainties about these mechanisms have fueled a wealth of theoretical models. These include: models based on frustrated rotation [57, 58] and Erigen micropolar fluid theory [59]; attempts to adapt kinetic theory using granular temperature [60] or density-dependent [61–64] viscosities; extensions of kinetic theory incorporating a quasi-static stress at the internal friction angle of the material [65–70]; Ginzburg-Landau formulation of a fluid-solid mixture [71–73]; and other models based on chain-forces [74], activated processes [75] or "granular eddies" [76].

Several of the above-mentioned models conjecture jamming mechanisms–frustrated rotations, chain forces, granular eddies–which are, by construction, specific to granular materials. Our approach rests on the opposite viewpoint that, since jamming is observed in many amorphous systems, it is likely that it has a common origin. If this is the case, the specificities of grain-grain interactions should be weakly relevant, and simple hard-sphere models of granular interaction should be sufficient in first approximation. It was thus proposed [1] that a rescaling of the dynamics of perfectly hard granular materials would allow to map their properties onto more usual glass formers. Building on the analogy between granular material and metallic glasses thus provides a local mechanism of jamming on the basis of the Shear Transformation Zone theory of plasticity [2, 3].

The present paper builds on the constitutive equations proposed in [1]: our goal is to test the microscopic assumptions underlying the STZ formulation of constitutive equations for granular materials and test the predictions of the theory. To proceed in this direction we first test whether dense granular flows are describable as a local phenomenon, governed by local hydrodynamic equations, or must be treated as a global problem, thereby relying upon the emergence of long-range correlation through mechanisms such as force chains. For this purpose, we have implemented contact dynamics simulation of sheared granular materials in two different configurations: (i) simple shear in a periodic cell which grants direct access to time- and space-averaged constitutive relations between various quantities including strain rate, stresses, granular temperature (ii) thick flows of granular material down an incline plane, which are compared with the measurements performed in simple shear. Next we reproduce in our numerical system of granular materials observations of non-affine displacement first made by Falk and Langer in Lennard-Jones glasses. This observation provides further grounding for the analogy between granular materials and common glass-formers and direct support for the relevance of STZ theory to granular materials. The construction of STZ constitutive equations for granular flows will follow and finally a fit of the theory with our numerical data.

The plan of our paper is as follows. We first present equations of motion in the mathematical limit of perfectly hard grains, discuss their invariance, how it is related to granular temperature, and why the results for perfectly hard grains are applicable to natural and experimental granular materials. Secondly we construct our numerical test, provide algorithmic details, and compare the rheology of a dense granular materials in a periodic cell and down an incline plane. Then we present Falk and Langer's STZ theory before showing how it adapts to granular materials, and conclude with fits of our data.

I. FUNDAMENTAL RESULTS FOR PERFECTLY HARD GRAINS

When grains are dry–so that no water bridges induce attraction–and of size larger than the micrometer scale–so that no electrostatic interaction intervenes–their interaction is purely repulsive: it results from the elastic deformation of grains at contact and the dissipation of energy during collisions and via friction. The complexity of this interaction calls for a first question: which properties of the grain-grain interaction contribute to certain macroscopic observations? In some instances, details of the grain-grain interaction seem critical: for example, the Hertzian repulsion [14] is essential to understand the acoustic properties of granular materials [**?** **?**]. Numerical implementations of granular materials have thus relied on more or less elaborate models of the grain-grain interaction [77, 78].

We are concerned here by dense flows of granular materials and, in particular, flows down inclines as found in the experiments by Pouliquen [79] and numerics by Silbert and coworkers [26, 28]. For these dense granular flows a recent study by Campbell helps us assess the importance of the elastic (soft) part of the repulsive potential [80] versus the limit in which grains appear as perfectly hard spheres. Campbell presented a detailed analysis of the different flow regimes obtained in a three dimensional simple shear of dense granular flows when varying the stiffness k of the repulsion, the shear rate $\dot\gamma$, and the mass density ϕ. He found that the dimensionless parameter $\Upsilon \equiv \frac{k}{\phi D^3 \dot\gamma^2}$, where D is the grain size dictates the character of the flow: for $\Upsilon < 10^5$ the stresses depend sensitively on the value of Υ whereas for $\Upsilon > 10^5$ the stresses do not depend on Υ. The mathematical limit of perfectly hard spheres corresponds to Υ approaching infinity. This means that if $\Upsilon > 10^5$ for the granular shear flow of interest then approximating the interaction in terms of perfectly hard grains is acceptable. In a realistic flow, Campbell estimates that $\frac{k}{\phi d} \approx 10^4\,\mathrm{m}^2\mathrm{s}^{-2}$ so that, assuming particles of size 1 mm, the shear rate would have to reach a value greater than $1000\,\mathrm{s}^{-1}$ in order for $\Upsilon < 10^5$. Thus, for realistic flows we have $\Upsilon > 10^5$. As a consequence of this analysis, we can conclude that most experimental and natural flows of granulates are in the limit where the soft part of the repulsion is entirely masked by the steric exclusion: to study these flows, it is sufficient to consider properties of perfectly hard grains. In the following sections we explore how the mathematical limit of perfectly hard spheres gives insight into fundamental processes which, through the argument by Campbell, relate to most all experimental shear flows.

Equations of motion and Hard Sphere conditions

The motion of N spherical grains in a d-dimensional granular material is determined by Newton's equations for the positions q_i, angular orientations θ_i, momenta p_i and angular velocities ω_i

$$\frac{dq_i}{dt} = \frac{p_i}{m_i}, \quad \frac{dp_i}{dt} = \sum_j F_{ij} + F^{ext}, \tag{1}$$

$$\frac{d\theta_i}{dt} = \omega_i, \quad \frac{d\omega_i}{dt} = \frac{1}{I_i}\sum_j R_i \hat{n}_{ij} \times F_{ij}, \tag{2}$$

where F^{ext} represents an external force such as gravity, F_{ij} represents a contact force on grain i by grain j, $\hat{n}_{ij}$ is the unit normal vector pointing from grain i to grain j, R_i is the radius of grain i, and I_i is the moment of inertia.

These equations must be complemented with a prescription for the contact forces. In the hard sphere limit these contact forces are determined self-consistently by the conditions that there is no penetration between grain–a force is instantaneously created upon contact to impede penetration and remains non-zero until the contact is broken–and by the friction law which couples to rotational degrees of freedom.

Important properties of granular materials arise directly from an invariance of the equations of motion (1, 2). We now spend some time to study these properties and assess their consequences for macroscopic observations, in particular Bagnold's scaling.

Bagnold's scaling

The success of kinetic theory came in a large part from its ability to account for the scaling between stress σ and strain rate $\dot{\gamma}$ ($\sigma \sim \dot{\gamma}^2$) first observed by Bagnold in dense granular materials. In Bagnold's experiment, the strain rate was set and the stress measured. The original argument given by Bagnold [23] relied on the assumption that the stress measured in his experimental resulted solely from binary collisions: the frequency of collisions and momentum change per collision is proportional to the shear rate, therefore the stress is proportional to the square of the shear rate.

Recent works have introduced puzzling information to this issue. On the one hand, the observations by Bagnold have been criticized: they may have arisen from a secondary instability of the granular flow in his shear cell [25]. On the other hand, Bagnold's scaling has been directly observed by measuring shear stress and strain rate profiles in numerical simulations of granular flows down inclines [26, 28], and is found to be consistent with experimental observations of the average flow rate in the same geometry [79].

Although kinetic theory has succeeded in theoretically explaining the origin of Bagnold's scaling, the derivation relies on the assumption that all interactions between grains occur through binary collisions. This assumption is applicable to the regime of rapid collisional flows but is not upheld for dense flows, such as those originally studied by Bagnold, and a new argument must be formulated for this flow regime.

We contend that in both the dense and collisional flow regimes Bagnold's scaling arises from a very fundamental invariance of Newton's equations in the hard sphere limit, which does not require any of the assumptions of kinetic theory to hold. Namely, for a granular material free from external forces, the time evolution will obey equations (1, 2) with $F^{ext} = 0$. If we now rescale the contact forces by a scalar value $F_{ij} \to F_{ij}/A$ and simultaneously rescale the time $t \to t\sqrt{A}$ then Newton's equations are transformed to read

$$\frac{dq_i}{dt} = \frac{p_i^{new}}{m_i}, \quad \frac{dp_i^{new}}{dt} = \sum_j F_{ij}, \tag{3}$$

$$\frac{d\theta_i}{dt} = \omega_i^{new}, \quad \frac{d\omega_i^{new}}{dt} = \frac{1}{I_i}\sum_j R_i \hat{n}_{ij} \times F_{ij}, \tag{4}$$

where $p_i^{new} = p_i/\sqrt{A}$ and $\omega_i^{new} = \omega_i/\sqrt{A}$. This form for Newton's equations is identical to (1) and (2) with new values for the momenta and angular velocities.

Under the rescaling of contact forces and time, the positions and angular orientations remain unchanged, while the velocities are changed according to the time rescaling. If we were to watch a movie of one granular flow where the grains have initial velocities p_i, ω_i and watch another movie at half the speed where the initial velocities are doubled $p_i \to 2p_i$, $\omega_i \to 2\omega_i$, the two movies would look exactly the same. The difference in the dynamics is that the contact forces measured in the second movie would be 4 times larger than those in the first movie.

This invariance is a property of *perfectly hard grains* which must hold in the inertial regime, even infinitely close to jamming, when multi-body interactions dominate over collisional terms and the basic assumptions of kinetic theory fail. In an experiment, this scaling breaks down only when it is no longer appropriate to model the experimental system by perfectly hard grains. From the arguments of Campbell introduced earlier, most all experimental granular flows are in the regime where it is appropriate to model the system by hard grains.

Granular temperature

Because the positions and angular orientations of grains are invariant to a change in time and force scales, the path that a granular material takes in configuration space is also invariant: only the speed along this path is altered. The path that a granular material takes in configuration space can thus be separated from the rate at which events occur along that path.

This observation leads to a natural definition of granular temperature T: the rate at which microscopic events occur on the configuration space path is defined as $\sqrt{T}/\langle R\rangle$ (the average grain size $\langle R\rangle$ is inserted so that T has units of velocity squared). These microscopic events are not necessarily collisions, but can also be understood as force fluctuations or minute displacement of grains allowing for propagation of "hard-sphere" noise.

This invariance is directly related to the structure of Newton's equations and the existence of inertial terms–or accordingly, to the fact that kinetic energy, no matter how small, is well defined. The granular temperature defined above as a "velocity" along phase space trajectories is thus naturally proportional to kinetic energy:

$$T_k = \frac{\langle m\rangle}{2}(\langle v^2\rangle - \langle v\rangle^2) + \frac{\langle I\rangle}{2}(\langle \omega^2\rangle - \langle \omega\rangle^2), \qquad (5)$$

where m is the mass, v the velocity, I the moment of inertia, ω the angular velocity, and brackets denote a spatial average. Since the granular and kinetic temperatures are defined up to a constant factor, we will identify them. It means that at any time, the kinetic energy provides an estimate of the frequency of elementary events in a multicontact system.

What quasi-static limit?

Let us now consider a uniform granular material in simple shear flow. If we imagine changing the force and time scales then the invariance in Newton's equations guarantees that the dynamics will remain unaltered: only resulting in new velocities that are determined from the time rescaling. However, under the rescaling, quantities such as the pressure and strain rate will take on different values. The quantities of interest are those that are invariant to the transformation. These quantities must be formed of ratios of force scales, ratios of time scales, or ratios of force to time scales. Denoting p and σ the pressure and shear stress, $\dot\gamma$ the strain rate, ϕ the mass density and D the average diameter of grains, the invariant (and dimensionless) quantities are: $\frac{p}{\phi\, D^3\, \dot\gamma^2}$, $\frac{\sigma}{\phi\, D^3\, \dot\gamma^2}$, $\frac{p\, D^{d-1}}{T}$, $\frac{\sigma\, D^{d-1}}{T}$, $\frac{T}{\phi\, D^{d+2} \dot\gamma^2}$, and $\frac{\sigma}{p}$, which must be single valued functions of *density* only (independent of the strain rate). This observation, established by the invariance in Newton's equations which holds for granular flows in the dense and collisional regimes, automatically predicts Bagnold's scaling: since $\frac{\sigma}{\phi\, D^3\, \dot\gamma^2}$ is a function of density only, then $\sigma \propto \dot\gamma^2$.

This leads to a simple, yet remarkable property: there is no quasi-static limit for perfectly hard grains. *At a given density*, changing the strain rate does not lead the system toward any different regime or "phase". The material does not go closer to jamming because the strain rate is scaled down: the system is always exploring the same trajectories, in phase space, but at a slower speed. This is exemplified by the jamming phase diagram of granular materials [27] where changing the density allows the granular material to jam, whereas changing the strain rate does not.

The scaling invariance is also directly related to the observation by Campbell that "there is no path between inertial (rapid) flow and quasi-static flow by varying the shear rate at fixed concentration" [80]. This is no surprise once we understand this invariance of Newton's equations for perfectly hard grains: only two regimes are accessible, jammed or inertial, and density is the parameter which changes the statistical properties of a flow of perfectly hard grains.

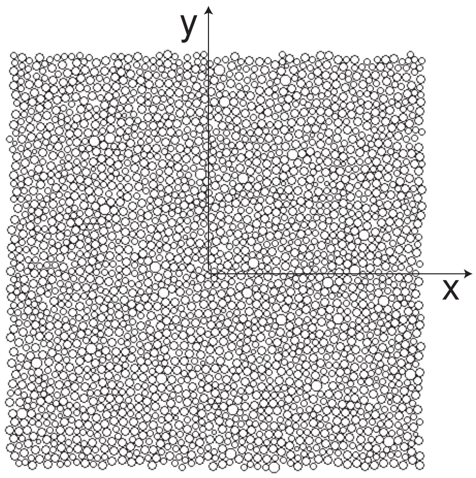

FIG. 1: Snapshot of a granular material simulation in the simple shear configuration. Each grain has an average velocity in the x-direction given by $\dot\gamma y$, where $\dot\gamma$ is the strain rate. The center of the cell is defined as $x = y = 0$.

II. CONSTRUCTION OF A NUMERICAL TEST

Before addressing questions which are specific to the STZ formulation of constitutive equations for granular materials, we wish to clarify one major issue for the relevance of constitutive equations: we want to observe stress-strain relations when granular temperature and stresses are appropriately scaled, show that it compares well with very standard responses of yield stress fluids, and show that the local rheology measured in simple shear matches with the bulk rheology of a granular flow down an incline.

In order to address these issues, we implemented numerical simulations of granular materials in two different geometries:

- We implemented simple shear in a cell with Lees-Edwards (LE) boundary conditions. In this configuration, the density and the shear rate is prescribed. The simulation cell is, by construction, translation-invariant. It grants direct access to averaged quantities: granular temperature, and components of the stress tensor. Using this configuration, we can thus characterize the steady relation between stresses, granular temperature and strain-rate and extract numerically the parameters of a constitutive laws for granular materials. A picture of this shearing geometry is shown in figure 1.

- We implemented a granular flow down an inclined plane made of stationary grains. The simulation cell is periodic in the direction (x) parallel to the plane; the flow is inhomogeneous in the perpendicular (y) direction. In this configuration, the stresses

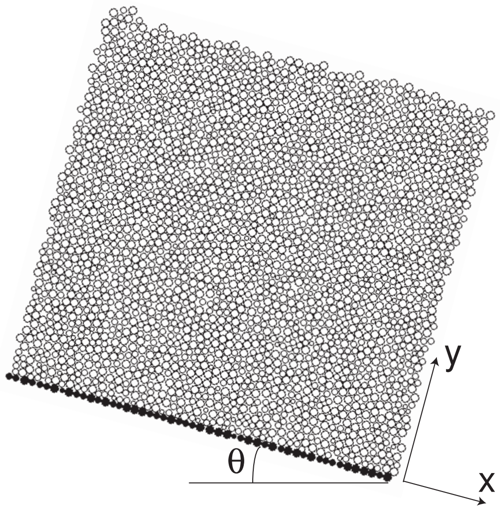

FIG. 2: Snapshot of a granular material simulation in the incline flow configuration. Grains create a stationary incline at angle θ on which the flowing grains are accumulated and allowed to flow. Gravity forces the particles and is directed vertically downward.

are prescribed by the angle of the incline. We perform x-averaged, y-dependent measurements of granular temperature, velocity profiles and strain-rate. Large heights of the granular layer grant access to the bulk rheology of the flow: this permits (i) to check the existence of a well-define bulk rheology in the large height limit, (ii) to compare it with the measurements in simple shear. A picture of this shearing geometry is shown in figure 2.

In order to permit a quantitative comparison of both experiments, we use the same material: a two-dimensional polydisperse mixture of constant density grains with the radii drawn from a flat distribution with average radius $\langle R\rangle$ and full width σ. For all the simulations in this paper, we set $\sigma/\langle R\rangle = 0.5$, using $\langle R\rangle = 0.7$. This distribution prevents crystallization and produces an amorphous granular material, as can be seen from measurement of the pair correlation function in figure 3. The horizontal axis (d) in this figure corresponds to the distance between a pair of grains, divided by the sum of their radii. This normalizes the figure so that $d = 1$ corresponds to contacting grains. Other than this peak, the function has a variation (which implies a correlation) between $d = 1$ and $d = 3$. There is no correlation beyond $d = 3$. Because there is no large scale correlation, this implies that the granular material is amorphous.

In this paper, we present data for zero normal and tangential coefficients of restitution $e_n = e_t = 0$: it was shown by Moucheront et al [?] that the regimes reached by granular materials are almost independent of e below some threshold around $e \sim 0.7$. Different friction coefficient have been used: frictionless grains and $\mu = 0.4$.

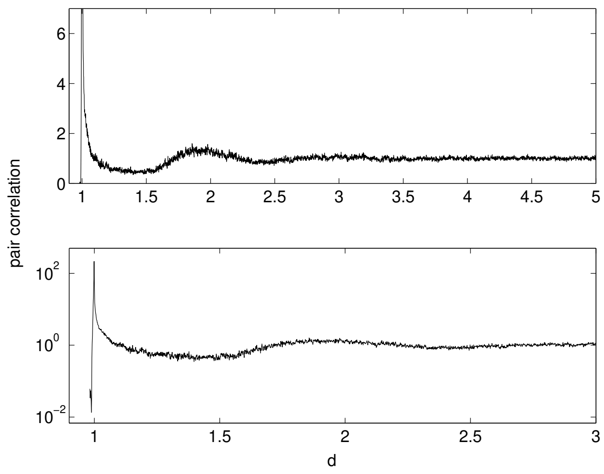

FIG. 3: The pair correlation function for a frictionless granular material at high density in linear (top) and log (bottom) scales. This function is representative of the pair correlation functions for other densities and for granular materials with friction between grains. There is a large peak at the for contacting grains ($d = 1$) and some variation between $d = 1$ and $d = 3$. For $d > 3$ there is no correlation between grains. This implies that the material is amorphous.

Our implementation of the granular material rely on the contact dynamic algorithm [81–85]. We refer to the literature for technical details and present below a brief overview of the method, supplemented by a single addition we made in order to construct a Lees-Edwards simulation cell for frictional granular materials.

Contact Dynamics

Contact Dynamic algorithms were constructed to carry out numerical simulation of spheres interacting through the enforcement of hard sphere conditions [81].

When a contact occurs there is an non-continuous force created that restricts the grains from penetrating. The magnitude of this force is chosen to ensure that the final relative velocity u of the grains is related to the initial relative velocity u^0 via the equations

$$u_n = -e_n u_n^0 \quad u_t = e_t u_t^0 \tag{6}$$

where e_n, e_t are constant restitution coefficients that will depend on the shape and consistency of the grains, and the n, t subscripts represent the normal and tangential parts of the relative velocity with respect to the contact. At each timestep, the algorithm computes the contact forces by first ensuring that these relations hold at each contact. To include friction, the Contact Dynamics algorithm ensures that the resulting tangential force F_t is less than or equal to μF_n where μ is the friction coefficient and F_n is the normal force. If this constraint does not hold, then the algorithm sets $F_t = \mu F_n$ in order to comply with Coulomb friction.

In this way the Contact Dynamics algorithm calculates at each time step contact forces which are consistent with Newton equations and the hard sphere contact law.

SLLOD equations for simple shear flow

Lees-Edwards boundary conditions permit us to prescribe the deformation of a material by controlling the positions of the image cells [86]. In all of the simulations presented here, we impose a constant strain rate $\dot{\gamma}$ in the y-direction so that a grain at position y has an average velocity of $\dot{\gamma} y$ in the x-direction (see figure 1).

It was recognized in early implementations of LE boundary conditions that when deformation is applied through the cell images only, the information needs time to propagate from the cell boundaries to its center. In order to ensure rapid propagation of this information and prevent the boundaries between cells to play any particular role –which guarantees translation invariance–it is necessary to modify the Newton equation by introducing so-called SLLOD terms. These terms can be understood as a sort of "shear bath", with all particles in the cell being directly coupled to the overall deformation [87]. These equations introduce a mechanical perturbation in the equations of motion that gives each grain an average velocity consistent with simple shear flow. If we separate the momentum p_i of each grain i into the average part $m_i \dot{\gamma} y_i$ and fluctuating part $\tilde{p}_i$ so that $p_i = m\dot{\gamma} y_i + \tilde{p}_i$ then the SLLOD equations read:

$$\frac{dq_i}{dt} = \frac{\tilde{p}_i}{m_i} + \hat{x}\dot{\gamma}(q_i \cdot \hat{y}), \quad \frac{d\tilde{p}_i}{dt} = \sum_j F_{ij} - \hat{x}\dot{\gamma}(\tilde{p}_i \cdot \hat{y}). \quad (7)$$

The equation for the position q_i is simply the result of writing the momentum in terms of an average and fluctuating part whereas the equation for $\tilde{p}_i$ contains a new term $\hat{x}\dot{\gamma}(\tilde{p}_i \cdot \hat{y})$ which forces the shear flow. Since every grain in the primitive cell is acted upon by this mechanical force, the constant strain rate is imposed on all of the grains simultaneously at the beginning of the simulation. Furthermore it can be proven that in the Lees-Edwards geometry, the SLLOD equations give an exact representation of simple shear flow arbitrarily far from equilibrium [87, 88].

For a granular material with non-zero friction coefficient μ, the equations of motions should incorporate rotations of the grains (for $\mu = 0$ the tangential force is always zero and there is no rotation). It is expected that an SLLOD term should arise in the equations of motion for the peculiar angular velocity since, in the linear velocity profile indicative of simple shear flow, the top and bottom of every grain should be moving with slightly different velocities. This should give each grain an average rotation of $\dot{\gamma}/2$ which must be incorporated in equation (2) just as the average velocity $\hat{x}\dot{\gamma}(q_i \cdot \hat{y})$ was incorporated in equation (7). This leads to the following equations:

$$\frac{d\theta_i}{dt} = \tilde{\omega}_i + \frac{\dot{\gamma}}{2}, \quad \frac{d\tilde{\omega}_i}{dt} = \frac{2}{m_i r_i^2} \sum_j R_i \hat{n}_{ij} \times F_{ij} \quad (8)$$

where $\tilde{\omega}_i$ describes the peculiar angular velocity of grain i (total angular velocity subtracted by the overall shear flow angular velocity) and we have inserted the moment of inertia of constant density disks in two dimensions.

Equations (7) and (8) now give an exact representation of simple shear flow for a frictional granular material arbitrarily far from equilibrium.

This procedure simulates a sheared granular material with a constant shear rate. Couette flow experiments on granular materials do not always yield a constant shear rate: there is generally a region of the granular material that is moving at constant shear rate and this region accounts for the most motion, with the rest of the material being effectively jammed. Although our simple shear simulations do not capture all of the complexity of an actual Couette flow experiment, they are able to imitate the region that produces the most flow.

Macroscopic Quantities

We define the stress tensor $\Sigma^{\alpha\beta}$ via Cauchy's equation

$$\phi \frac{d}{dt}\langle v^\alpha \rangle + \phi \partial_\beta \langle v^\alpha \rangle \langle v^\beta \rangle = -\partial_\beta \Sigma^{\alpha\beta} + f^\alpha_{ext} \quad (9)$$

where $\langle v^\alpha \rangle$ is the average velocity in the α direction (averaged over grains), ϕ is the mass density, and f_{ext} is the external force per volume. Cauchy's equation simply states that the total time derivative of the average velocity (lhs) is proportional to the divergence of the stress tensor. Cauchy's equation thus gives a definition of the stress tensor from which there exists a procedure to derive the functional form of the stress tensor. This is called the Irving-Kirkwood derivation [88] and it yields

$$\Sigma^{\alpha\beta} V = \sum_i m_i (v_i^\alpha - \langle v_i^\alpha \rangle)(v_i^\beta - \langle v_i^\beta \rangle) + \sum_{i>j} (R_i + R_j) \hat{n}^\alpha_{ij} F^\beta_{ij} \quad (10)$$

where v_i is the velocity of grain i and V the volume of the granular material. This symmetric stress tensor can be written in terms of three variables: the pressure p, shear stress σ, and first normal stress difference N_1 defined as

$$\Sigma^{\alpha\beta} = \begin{pmatrix} p\,(1+N_1) & -\sigma \\ -\sigma & p\,(1-N_1) \end{pmatrix} \quad (11)$$

where the signs are chosen so that shear stress and pressure are positive in our conventions.

The granular temperature T is measured as

$$T=\sum_i v_i^2-\left(\sum_i v_i\right)^2+\frac{1}{2}\sum_i R_i^2\omega_i^2-\frac{1}{2}\left(\sum_i R_i\omega_i\right)^2 \tag{12}$$

which is proportional to the kinetic temperature from equation (5), with the factor of 1/2 coming from the moment of inertia calculated for constant density discs.

Lastly, for all of the numerical data that will be presented, we quantify the density of the system by its packing fraction ν. The packing fraction is defined as the area occupied by grains divided by the total area of the system. Packing fraction is proportional to both the mass density ϕ ($\phi = 4\nu/\pi$) and the number density n ($n = \nu/(\pi\langle R^2\rangle)$) in our simulations.

III. TEST OF LOCAL RHEOLOGY

We first study of the average relation between pressure p, shear stress σ, shear rate $\dot\gamma$, and granular temperature T in simple shear, using the periodic and translationally invariant LE cell. Next we compare these results with data obtained for the granular flow down an inclined plane.

Simple Shear

Preliminary test

In all of the simple shear simulations presented here we have simulated 2500 grains in a square primitive cell, although we have conducted a limited number of simulations with up to 10000 grains to ensure the accuracy of our observations. Because the contact dynamics algorithm induces some amount of numerical noise, the motion of a collection of grains driven at different shear rates are not expected to reproduce exactly the same phase space trajectory when changing the shear rate. In figure 4 we show sample data of the pressure and shear stress, as function of shear strain (strain rate multiplied by time) at a packing fraction of 0.8 with no friction and at four different values of the shear rate.

The stresses have been normalized by $\dot\gamma^2$ to emphasize the scaling expected to hold due to the invariance in Newton's equations which predicts that $p\dot\gamma^{-2}$ and $\sigma\dot\gamma^{-2}$ should not depend on $\dot\gamma$. We see that the data for different values of $\dot\gamma$ are identical at the beginning of the deformation, that is before numerical noise drives the system to different trajectories in phase space. The numerical noise disrupts the perfect invariance at a shear strain of approximately 2. For larger values of shear strain, the scaling still holds statistically. This test ensures that the simulations we conduct respect the invariance in Newton's equations for hard spheres.

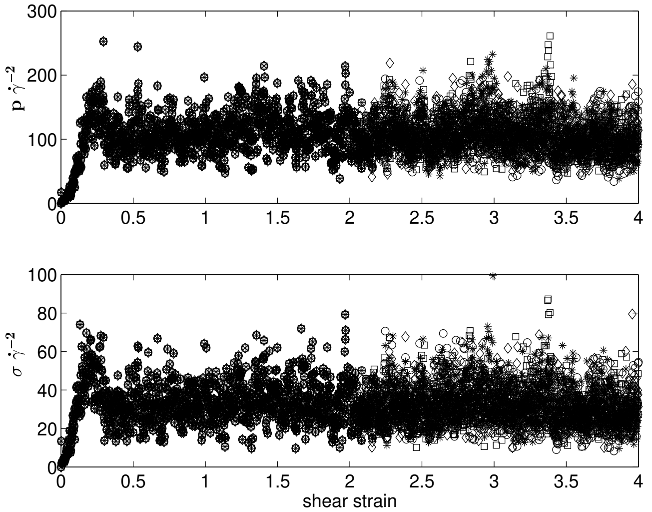

FIG. 4: (color online). Normalized pressure (top) and shear stress (bottom) as a function of total shear for four different shear rates γ of 100 (diamonds), 10 (squares), 0.1 (stars), and 0.01 (circles). Each quantity is normalized by $\dot\gamma^2$ which collapses the data on to two master curves, as predicted by the invariance for hard sphere systems.

For a granular material with pressure p, shear stress σ, temperature T, and strain rate $\dot\gamma$, there are three independent invariant quantities: σ/p, $\dot\gamma/\sqrt{T}$, and T/p. In figure 5 we show values of these three independent invariant quantities as a function of shear strain for a frictionless granular material at packing fraction of 0.8 For all quantities, steady flow is reached by a shear of approximately 0.5, and we will subsequently provide stationary data by time-averaging our measurements between strains of 2 and 10. The values of σ/p and T/p fluctuate much more than $\dot\gamma/\sqrt{T}$. This is due to the fact that σ and p depend on the forces between grains, which are highly fluctuating in the hard sphere limit. In our simulations with 10000 grains we observe that the fluctuations decrease while the average value remains constant, which suggests that in the large system size limit the fluctuations would disappear.

Liquid-solid transition

In figure 6 we present the steady state values of $p\dot\gamma^{-2}$, $\sigma\dot\gamma^{-2}$, $T\dot\gamma^{-2}$, and σ/p in simple shear for a range of high packing fraction systems that we have studied, at zero friction. Although there is relatively little change in these quantities for small packing fraction, for packing fractions larger that 0.75 there is an orders of magnitude increase in the values of the stresses and granular temperature. Additionally, the functional form of the stresses and granular temperature changes from approximately exponential to a function that grows faster than

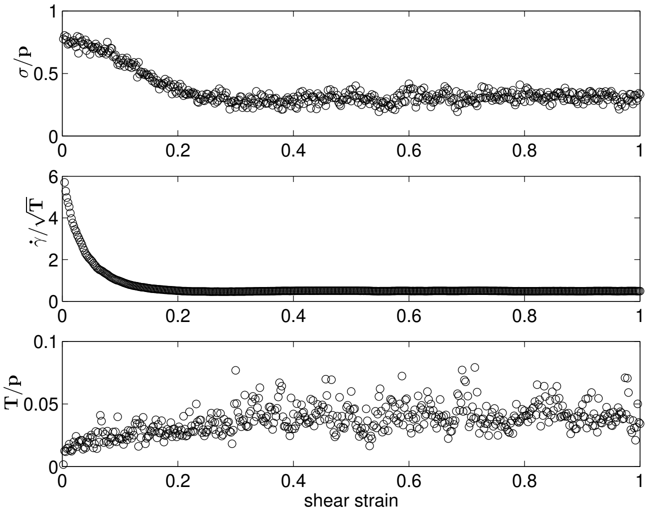

FIG. 5: Invariant quantities σ/p (top), $\dot{\gamma}/\sqrt{T}$ (middle), and T/p (bottom) as a function of shear strain for a frictionless granular material at packing fraction 0.8.

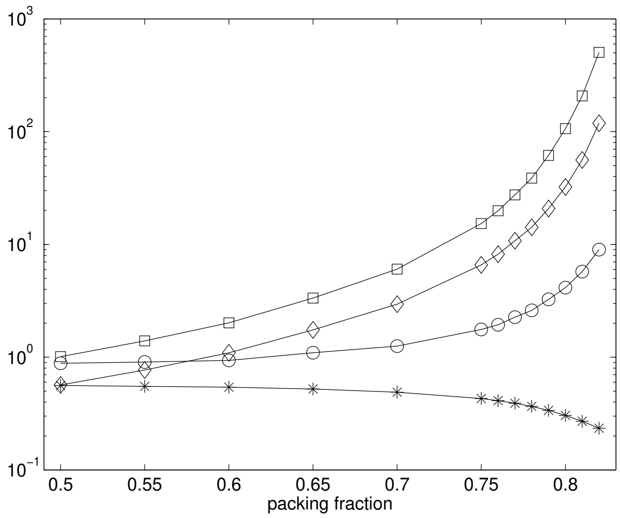

FIG. 6: Steady state values of $p\dot{\gamma}^{-2}$ (squares), $\sigma\dot{\gamma}^{-2}$ (diamonds), $T\dot{\gamma}^{-2}$ (circles), and σ/p (stars) as a function of packing fraction for a frictionless granular material.

an exponential at $\nu \approx 0.75$.

To better understand the increase in these quantities at large packing fraction we plot the static, collisional and kinetic components of the normalized pressure as a function of packing fraction in figure 7. We define the kinetic component of the pressure as one half the trace of the first term in equation (10) and the static component of the pressure is one half the trace of the second term in equation (10). The kinetic component arises from the velocity of the grains and the static component depends on the interaction between grains.

The collisional component of the pressure is defined as the portion of the static component arising from kinetic theory (it is calculated by assuming only binary collisions occur). For a binary collision between two frictionless grains labeled i and j with initial relative normal velocity u_n^0, the resulting impulse will be $I_{ij} = (1+e_n)m_r u_n^0$ where e_n is the normal coefficient of restitution and m_r is the reduced mass. This results in a force F_{ij}^c that is related to the impulse by $I_{ij} = \int F_{ij}^c dt$ and is only non-zero for grains at contact. Denoting the distance between the grains at contact as D_{ij}, the collisional pressure p_c is determined by summing $D_{ij}F_{ij}^c$ over all pairs of grains and integrating over a small shear strain step $d\gamma$:

$$\begin{aligned} p_c &= \frac{1}{2}\int \sum_{j>i} D_{ij}F_{ij}^c d\gamma \\ &= \frac{1+e_n}{2} \sum_{\text{contacts}} m_r u_n^0 \dot{\gamma} \end{aligned} \tag{13}$$

Since the first expression contains an integral over the contact force which is only non-zero for contacting grains, it can be replaced by the impulse multiplied by the strain rate, summed over the contacting grains only. The result follows. In our simulations with $e_n = 0$, the collisional component of the pressure simplifies to one half the reduced mass multiplied by the initial relative normal velocity of the contacting grains and the strain rate, summed over all contacts. If only binary collisions occurred then the collisional component would equal to the static component.

From figure 7 we see that for all packing fractions the collisional component of the pressure is less than or equal to the static component. For small packing fraction the value of the static part approaches that of the collisional part, but for large packing fractions the static part of the pressure is *orders of magnitude* larger than the collisional component: this is the regime, close to jamming, where the assumptions of kinetic theory fail. This signifies that the effects from clusters of grains become important in determining the pressure for dense flows and that interactions between grains can no longer be viewed as arising solely from binary collisions. Additionally, the functional form of the collisional pressure is approximately exponential for all values of packing fraction whereas the functional form of the static pressure closely mirrors the faster than exponential growth at large packing fractions seen in figure 6. These observations all strengthen the conjecture that for dense granular flows the interactions between grains is not strictly binary and that the interactions of grain clusters significantly modifies the stresses.

Alam and Luding [89] have measured the steady state values of the first normal stress difference N_1 in simple shear flow using a monodisperse collection of grains. In rapid flows, a non-vanishing value for N_1 results from collisional terms and the anisotropy in the distribution of velocities at Burnett order. [90] Alam and Luding reported that N_1 becomes negative at the onset of crystallization. We have thus measured the first normal stress

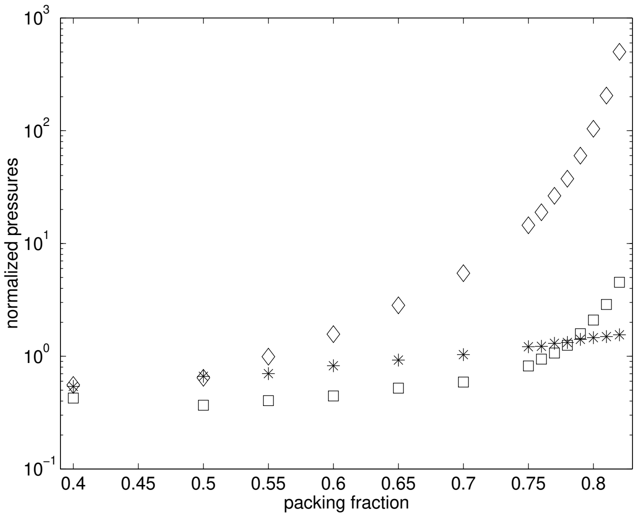

FIG. 7: Steady state values of the kinetic (squares), collisional (stars), and static (diamonds) components of the pressure as a function of packing fraction for frictionless granular materials, all normalized by dividing $\dot{\gamma}^2$. The magnitude of the static component of the pressure converges with the value of the collisional component for small packing fraction. We have included data from a low packing fraction system of 0.4 to illustrate this convergence. For larger packing fractions, the static component of the stress dominates and becomes orders of magnitude larger than the collisional component.

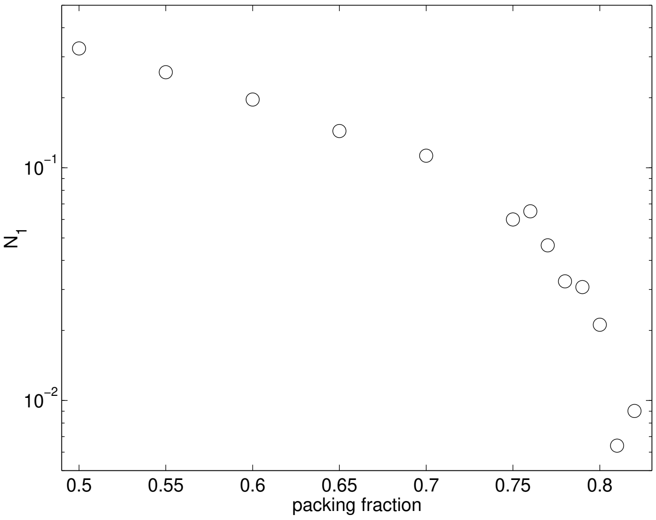

FIG. 8: First normal stress difference N_1 defined by equation (11) as a function of packing fraction for a frictionless granular material. $N_1 > 0$ for all packing fractions suggests that the granular materials are amorphous, and the decay of N_1 as a function of packing fraction reinforces the evidence from figure 7 that non-kinetic effects dominate at high packing fraction.

difference in our system in order to ensure the absence of crystallization and as a signature of the breakdown of kinetic effects. The observation in figure 8 that $N_1 > 0$ for all packing fractions in our system is consistent with the observation that our system remains amorphous. The decay of N_1 over all packing fractions is consistent with the statement that the kinetic effects become less important as the packing fraction increases, especially after $\nu \approx 0.75$ when it begins to quickly decay.

We see here that jamming is a complex process: first, in some cross-over region, the static part of the stress tensor begins to dominate over kinetic and collisional terms. Then as density is increased further, the late stages of jamming are controlled by the variations of the static stress only since the kinetic and collisional contributions become negligible (see figure 7).

This observation departs from the generally accepted assumption that, close to jamming, the static stress is always equal to the internal angle of friction, or repose angle of the material; it is consistent, however, with measurement by Campbell et al [49].

Flow down and inclined plane

In the simple shear cell, the density and strain rate were specified, while stresses and granular temperature were measured. We now focus on the flow down an inclined plane which provides a complementary situation: stresses are specified by the choice of an angle of inclination and by the gravitational field, while profiles of velocity and velocity fluctuations are measured and grant access to profiles of strain-rate and granular temperature.

We report in figure 9 mass density, granular temperature, and $\dot{\gamma}/\sqrt{T}$ as a function of depth for the steady flow of a non-frictional granular material at an angle of 12° and for a total height of approximately 50 grains. We have conducted simulations with heights ranging between 25 and 100 grain diameters to ensure that our results do not depend on the size of the system.

We observe that, in the bulk central region of the flow, the packing fraction profile is uniform, the granular temperature is linear, and $\dot{\gamma}/\sqrt{T}$ is constant. These observations hold in our simulations for all angles where the granular flow reaches a steady state. We only use data from these steady state flows in this paper. These observations are consistent with previous observations by Chevoir et al [92] and Silbert et al [26, 28].

There are four quantities of interest for incline flows– p, σ, $\dot{\gamma}$, and T– and these lead to three independent invariant quantities $\dot{\gamma}/\sqrt{T}$, σ/p, and T/p. We observe in our simulations that all of these invariants are constant in the bulk of the incline flow. Therefore it is interesting to compare these constant values with the constant values obtained from simple shear simulations. In figure 10 we present how the constant values of σ/p, T/p, and $\dot{\gamma}/\sqrt{T}$ in the bulk of the flow depend on packing fraction and compare with our results from the simple shear cell. The fact that data from different shear flows fall on the same

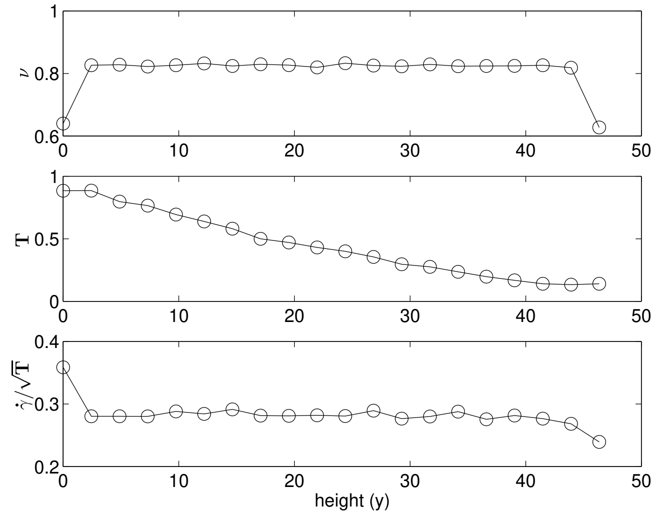

FIG. 9: Profiles of packing fraction (top), granular temperature (middle), and $\dot\gamma/\sqrt{T}$ (bottom) as a function of the height (y) in the pile, measured in grain diameters, for a non-frictional granular material at a 12° incline.

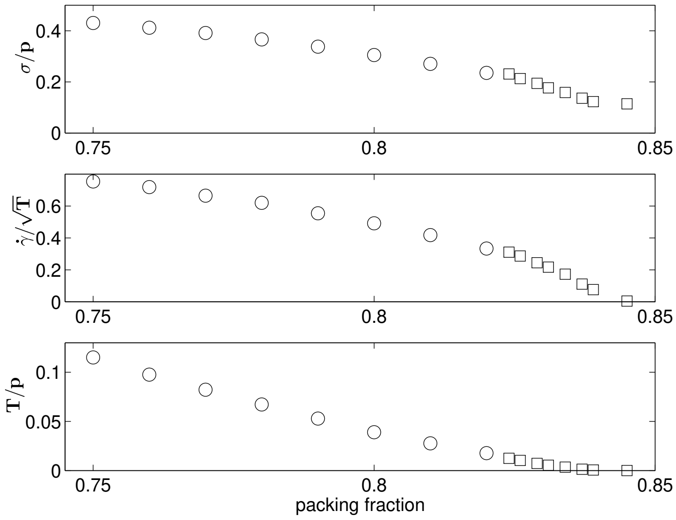

FIG. 10: The values of σ/p (top), $\dot\gamma/\sqrt{T}$ (middle), and T/p (bottom) plotted as a function of packing fraction. Data from simple shear flow (circles) and flow down an incline (squares) match on the same curves. This suggests that there is a local rheology that is independent of the particular shearing geometry.

curves is remarkable and suggests that one theory should be able to describe simple shear and incline granular flow.

Interestingly, the data from different flows do not overlap over a large interval of packing fraction: the flow down an inclined plane provides values at higher values of packing fraction than the simple shear cell. This due to (i) steady flows down an incline plane are more easily reached for lower inclinations, hence higher densities; (ii) the simple shear deformation is more difficult to integrate numerically at higher densities, because the periodic cell induces additional constraints that the contact dynamics manages with difficulty. Nevertheless, our use of two different configurations grants access to a broad range of $\dot\gamma/\sqrt{T}$, σ/p, and T/p; and the sets of data are consistent with the existence of a unique, local relation between them as apparent in figure 10.

Origin of a Local Rheology

The excellent agreement between the two sets of data is surprising in view of the belief that chain forces or non-local effects should arise in dense granular flow. Our observation come in direct contradiction with this idea and supports a very conservative opinion: that the motion of the grains decorrelates beyond some finite length scale, in accord with the fast decay of the pair correlation function (see figure 3).

As a consequence, in the bulk of the flow down an incline, it is possible to view layers of granular materials as effective simple shear cells. Such a layer of granular material, at depth y, responds essentially as if it was confined in a simple shear cell, in the absence of body forces, with sustained external stresses $\sigma(y)$ and $p(y)$. Of course the invariance in Newton's equations, which holds exactly for the simple shear cell, is slightly broken by the gravitational force field. However, deep in the bulk of the flow, large confining stresses eventually dominate over the gravitational field. This approximate invariance suffices to explain that Bagnold's scaling must hold for deep flows and explains the numerical data by Silbert and coworkers [26, 28].

More specifically, body forces are gradients of the stress tensor from Cauchy's equation (9): hydrodynamic equations are expected to arise when the gradients of macroscopic variables become small compared to the macroscopic variables themselves. What is surprising, however, is that the locality of the rheology is observable for the moderate heights that we can access in our numerical simulations. We believe that the reason why the hydrodynamic regime seems to be observed at such reasonable scales is the following: (i) the relevance of hydrodynamics limit depends on how macroscopic quantities, say Ψ, compare with $\ell\nabla\Psi$, where ℓ is a length-scale (ii) ℓ is not the size of the grain or a cluster of grains: it is the size of the region sampled by a given grain per strain unit, which is of the order of the mean-free path. Since for a dense granular material $\ell/\langle R\rangle << 1$, the validity of the hydrodynamic limit should hold over moderate heights.

As we will see, our theory provides constitutive equations which relate the static friction coefficient σ/p to the ratio $\dot\gamma/\sqrt{T}$. Anticipating the following sections, we present in figure 11 a plot of σ/p versus $\dot\gamma/\sqrt{T}$. As we will argue, such a plot is expected to be the granular counter-

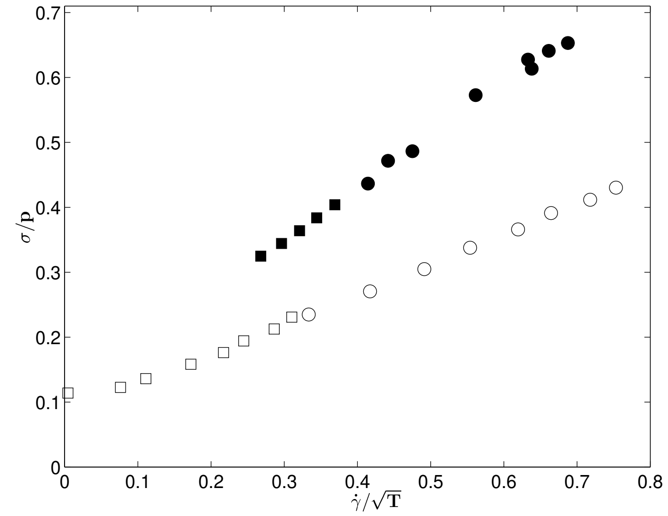

FIG. 11: σ/p plotted against $\dot{\gamma}/\sqrt{T}$ in steady state simple shear flow (circles) and incline flow (squares). Filled symbols correspond to frictional granular materials with coefficient of friction $\mu = 0.4$ and open symbols correspond to non-frictional granular materials with $\mu = 0$.

part of a stress versus strain rate plot for a glassy material [1], with the shear stress normalized by the pressure and the strain rate normalized by the granular temperature. We see here that the analogy is striking: when rescaled properly the granular material presents typical features of normal yield stress fluids [91]. For large values of normalized strain rate, the normalized stress is proportional to the normalized strain rate. For small values of the normalized strain rate, the linear relationship no longer holds and there is a yield (normalized) stress at zero (normalized) strain rate.

IV. CONSTITUTIVE EQUATIONS

Several conspicuous elements stem from the preceding observations: (i) the invariance of Newton's equations indicate that for a given density only invariant quantities are relevant to describe the state of a granular flow (ii) when invariant quantities are considered the granular material displays a "normal" rheology of a yield stress fluid (iii) the rheology measured in the Lees-Edward cell seem to extrapolate to the rheology measured from bulk data of a flow down an inclined plane.

These observations foster our hope to construct local constitutive equations for dense granular materials. Yet, before addressing the specificities of the STZ formulation of constitutive equations, we wish to argue that the scaling invariance of Newton's equations calls for a parallel scaling form of the constitutive equations.

Scaling form for constitutive equations

In general, constitutive equations should provide a relation between stresses and strain-rate, and a set of state variables $\{\psi_i\}$ which characterize the internal structure of the granular material. For granular materials the granular temperature T plays a quite specific role as a state variable; other state variables are expected to account for geometric properties of the granular packing.

Conservation of energy

Ogawa [93] was the first to recognized that in granular materials the temperature cannot be prescribed by a thermal bath, but rather it is set by energy balance. Kinetic theory provides estimates for the energy dissipation rate in dilute systems, hence providing approximations for the equation of motion which governs granular temperature. As a result, the notion of granular temperature has been tied to kinetic theory.

Granular temperature, however, is not reserved to the sole use of kinetic theory: it is relevant in all inertial flows since, as discussed previously, there is no quasi-static limit for hard-spheres, even infinitely close to jamming. In particular the dense flows of our simulations do not verify the assumptions of kinetic theory, yet in these inertial regimes kinetic energy is a perfectly relevant physical observable and is obviously set by energy balance.

At any time, the variation of kinetic energy results from the balance between external work done on the system and dissipative mechanisms. Because the system explores phase-space trajectories at a velocity proportional to $\sqrt{T}$, the rate of energy dissipation should scale as $\sqrt{T}\,T$: the square root gives the frequency of dissipative events and each event dissipates energy proportionally to T. Energy is introduced to the system via the external forcing with a rate of $\sigma\dot{\gamma}$. Therefore, the energy balance equation should be of the form

$$\phi\dot{T} = \sigma\dot{\gamma} - \alpha(\phi, \{\psi_i\})T\,\frac{\sqrt{T}}{\langle R\rangle} \tag{14}$$

with ϕ being the mass density. The factor α is a geometric factor: it depends only on the relative positions of the grains, but should not incorporate any further dependence on T or stresses. It should, in particular, depend on density ϕ and possibly on other state variables $\{\psi_i\}$ which characterize the geometrical structure of the granular packing. By scaling invariance, the steady state value of α should depend of ϕ only.

This equation is similar in form to the energy conservation equation derived in kinetic theory [94]. This is no surprise since kinetic theory must uphold the invariance of Newton's equations. Kinetic theory, provides an estimate for $\alpha(\phi)$, and it is possible that even in dense flows

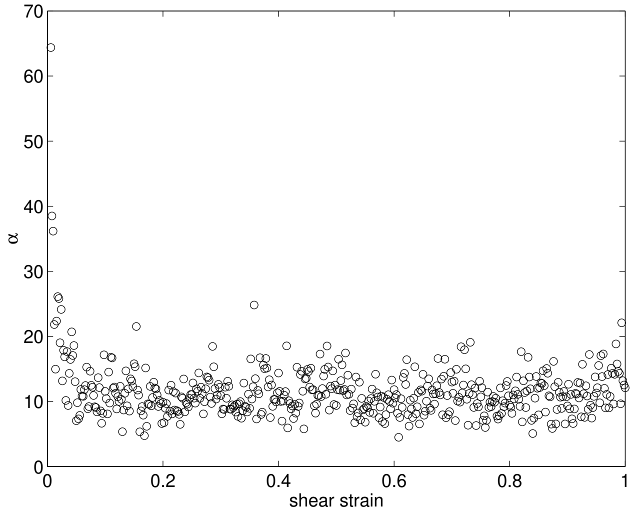

FIG. 12: α from equation (14) as a function of shear strain for a simple shear flow of a non-frictional granular material at packing fraction 0.8. For small values of shear, α varies slightly, but quickly becomes constant at a small value of shear strain.

this estimate remains reasonable for non-frictional grains because collisions are then the only events when energy is dissipated, even though multibody collisions may induce departure of this relation from predictions of kinetic theory.

In figure 12 we present a plot of α as a function of shear strain for a non-frictional granular material in simple shear flow, calculated via equation (14). Although α should be constant for all values of shear at a set density, we observe a dynamic in α at the start of the simulation. However this behavior quickly disappears and α becomes constant.

Constitutive relation

Since granular temperature is defined as the frequency of elementary events along phase-space trajectories, the strain rate should scale as

$$\frac{\dot{\gamma}}{\sqrt{T}} = f\left(\frac{\sigma}{p}, \frac{T}{p}, \psi_i\right), \tag{15}$$

where f denotes an unknown function and we assume that the state variables ψ_i are purely geometric: they depend neither on the amplitude of the forces nor on the instantaneous value of the granular temperature.

If we combine equation (15) with equation (14) in steady state where $\dot{T} = 0$, then we see that

$$\sigma = \left[\alpha F\left(\frac{\sigma}{p}, \psi_i\right)^{-3}\right]\dot{\gamma}^2. \tag{16}$$

so that Bagnold's scaling is upheld.

In the rest of this section we study the STZ formulation of constitutive equations and apply it to dense granular materials.

STZ theory

Basics

The Shear Transformation Zone (STZ) Theory of amorphous solids was proposed in [2, 3, 95–98] to account for the behavior of dense amorphous materials at low temperature. The theory is motivated by observations from simulations [99–104] and experiments [105] which suggest that plastic deformation in amorphous materials results from non-affine rearrangements of small clusters of particles [106]. Additionally, Falk and Langer were able to show that there exist different types of zones which present a preferential response to different orientations of shear forces. They suggested to introduce densities of these zones as state variables to characterize the internal structure of the molecular packing.

Central to the theory is the assumption that once an STZ undergoes an elementary rearrangement in a given direction it is unlikely that it can shear again in the same direction, although in can easily shear in the reverse direction. Therefore zones appear as two state systems and in the simplest version of the theory only two types of orientation (denoted $-$ and $+$) are chosen, aligned and anti-aligned with the shear. A rearrangement corresponds to a transition of a zone from a $\pm$-state into a $\mp$-state and vice-versa. The plastic shear rate is thus given by the rate at which STZs respond to external stresses:

$$\dot{\gamma} \propto R_+ n_+ - R_- n_-. \tag{17}$$

The rates $R_\pm$ are the stress-dependent probabilities that zones of $\pm$ types are transformed into one another.

This constitutive relation should be complemented with an equation of motion for the densities $n_\pm$, which is postulated to be of the form:

$$\dot{n}_\pm = R_\mp n_\mp - R_\pm n_\pm + w(a - b n_\pm). \tag{18}$$

The first two terms correspond to the transformation of STZs into their two possible states. The last term accounts for the fact that STZs are renewed by the overall macroscopic deformation: it contains a creation and destruction rate, both proportional to the plastic work w of external forces per time unit.

Observation of directional response

Before applying STZ theory to granular materials, we check that the same qualitative observations as in [2] can be performed in these systems, namely (1) that non-affine motion occurs in localized regions, and (2) that the positions of the localized regions depends sensitively on the orientation of the shear. The first observation motivates the choice of density of STZs as a state variable, and the second observation shows that each STZ has an orientation and therefore only responds to certain orientations of shear stress.

These observations are based on a measure of the non-affinity of the deformation of a cluster of a few molecules or grains, following [2]. Falk and Langer proposed the following criterion: the grains undergoing non-affine rearrangement can be determined by calculating, for each grain, the local strain rate at one time, and then measuring the difference D between the actual position at a later time and the position predicted from the local strain rate at the previous time. In practice, D is determined by minimizing

$$\tilde{D}^2(t,\Delta t) = \sum_n \sum_i \Big(r_n^i(t) - r_0^i(t) - \sum_j (\delta_{ij} + \dot{\gamma}_{ij}) \times \big(r_n^j(t-\Delta t) - r_0^j(t-\Delta t)\big)\Big)^2 \quad (19)$$

with respect to the shear rate $\dot{\gamma}_{ij}$, where the indices i and j are spatial coordinates and the index n runs over all grains in contact with the reference grain, labeled by the index $n = 0$. The minimum value of $\tilde{D}$, denoted D, is an approximation of the local deviation from affine displacement for the reference grain in the time interval $[t - \Delta t, t]$. If there is no non-affine motion, then the motion of each individual grain should be completely determined by a local shear rate and $D = 0$. If there is non-affine motion, then $D > 0$.

We have applied this test for non-affine motion to granular materials in simple shear to produce figure 13, which is the counterpart of figure 3 in [95] and figure 7 in [2]. Each picture has been created by shearing an identical initial arrangement of particles in a certain direction. D is the local measure of non-affinity obtained by comparison between the initial and final states. If D is larger than a reference value, the particle is said to have moved non-affinely and colored black.

We notice that the grains moving non-affinely tend to clump into localized regions. In figure 13 parts (a) the system is sheared from strains of 0 to 0.05, and in (b) the system is sheared to from strains of 0.1 to 0.15 and we notice that the size of the resulting non-affine regions is about the same in each picture. In (c) the system is sheared from strains of 0 to 0.15 and now the size of the non-affine regions increases, suggesting many more fundamental rearrangements of STZs in the larger time period. In (d) the system is sheared from strains of 0 to -0.05 (in the *opposite* direction), starting from the same initial configuration as in (a). Once again we observe that the non-affine regions tend to form clusters. However, in

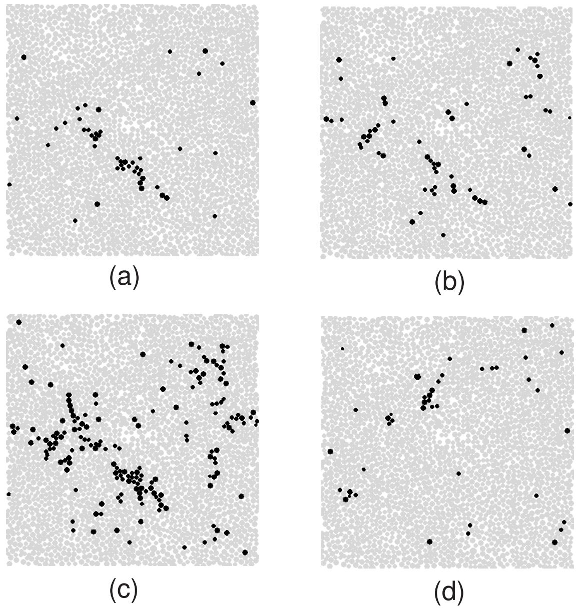

FIG. 13: Screenshots of granular materials in steady state simple shear flow with grains undergoing non-affine displacement colored black. In (a) the system is sheared from 0 to 0.05, in (b) the system is sheared from .1 to .15, in (c) the system is sheared from 0 to .15, and in (d) the system is sheared in the opposite direction, from 0 to $-.05$.

comparing (a) and (d) we notice that the size of the non-affine regions is about the same in the two figures, but the locations are different. If the regions undergoing non-affine displacement did not have an orientation we would expect non-affine motion to occur in the same location, regardless of the orientation of the stress. However this is not the case and the data in figure 13 suggests that the regions that move non-affinely have an orientation. This is qualitative evidence that the core assumptions of STZ theory are upheld in granular materials.

STZ Theory for Granular Materials

The STZ densities $n_\pm$ account for structural properties of a molecular or granular packing. They are thus expected to depend only on the positions of grains, orientations and distribution of forces, orientations of velocities, but not on the overall amplitude of the forces or amplitude of velocities. Following [1], these functions are determined using the invariance in Newton's equations. Since w represents the plastic work done on the system per unit time it should be proportional to $\sigma\dot{\gamma}$. In order to make w invariant, we normalize by pressure so that $w = \sigma\dot{\gamma}/p$. As for $R_\pm$, because of the invariance in Newton's equations, we can separate the rate at which an STZ attempts to rearrange from the probability that an attempt leads to a successful rearrangement. The attempt rate must be proportional to $\sqrt{T}$ which sets the microscopic event rate and the probability to rearrange is written as an exponential activation factor of the invariant form $e^{\pm\kappa\sigma/p}$. It then comes: $R_\pm \propto \sqrt{T} e^{\pm\kappa\sigma/p}$.

Combining the expressions for $R_\pm$ and w with equations (17) and (18), while making a change of variables from $n_\pm$ to $\Delta \propto n_- - n_+$ and $\Lambda \propto n_- + n_+$, yields the following equations:

$$\dot{\gamma} \propto \sqrt{T}\left(\Lambda \sinh\left(\kappa\frac{\sigma}{p}\right) - \Delta \cosh\left(\kappa\frac{\sigma}{p}\right)\right) \quad (20)$$

$$\dot{\Delta} \propto \dot{\gamma}\left(1 - \zeta\frac{\sigma}{p}\Delta\right) \quad (21)$$

$$\dot{\Lambda} \propto \dot{\gamma}\frac{\sigma}{p}(1-\Lambda). \quad (22)$$

Λ denotes the total number of zones and Δ measures the mismatch between zones of different orientations and therefore is related to the anisotropy of the granular packing. κ and ζ are constants that do not depend on the macroscopic variables $\dot{\gamma}$, T, σ, or p. However we would expect these constants to depend on properties of the grains such as shape, distributions of radii, restitution coefficients, friction coefficients, or other local static variables, including density.

Steady states

These equations present two types of steady state solutions [1–3]. One branch of solutions represents a jammed state: $\dot{\gamma} = 0$, and occurs when $\Delta/\Lambda = \tanh(\kappa\sigma/p)$. The other branch of solution represents the steady flow and occurs when $\Lambda = 1$ and $\Delta = p/(\gamma\sigma)$.

An elementary analysis of the phase diagram of this dynamical system indicates that the jammed state is stable iff

$$\zeta\frac{\sigma}{p}\tanh\left(\kappa\frac{\sigma}{p}\right) \leq 0 \quad (23)$$

and the flowing state is stable otherwise. The limit of stability occurs at a critical angle θ^*, which is thus the solution of:

$$\zeta \tan\theta^* \tanh(\kappa \tan\theta^*) = 0 \quad (24)$$

θ^* identifies as the repose angle of our granular material.

In the steady flowing regime ($\dot{\gamma} \geq 0$) STZ theory yields the following relation:

$$\frac{\dot{\gamma}}{\sqrt{T}} \propto \left(\sinh\left(\kappa\frac{\sigma}{p}\right) - \frac{p}{\sigma\zeta}\cosh\left(\kappa\frac{\sigma}{p}\right)\right) \quad (25)$$

In particular, in the limit when the ratio $\frac{\dot{\gamma}}{\sqrt{T}}$ vanishes, σ/p converges towards $\tan\theta^*$. Therefore the STZ theory accommodates cases where there is a residual pressure and shear stress at zero shear rate and predicts that in this case the shear stress will be proportional to the pressure.

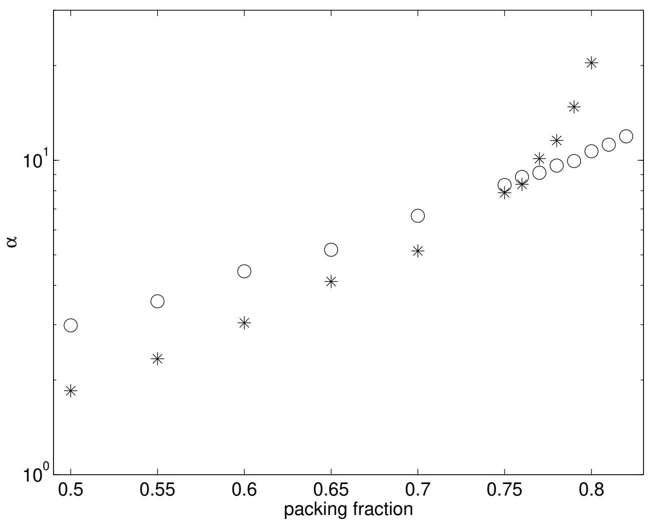

FIG. 14: Density dependence of α, defined through equation 14, for frictional (stars) and non-frictional (circles) simple shear flows.

Numerical tests

The constitutive equations for granular materials introduced in this paper are entirely specified by equations (14) and (22). We now compare the steady state relations predicted by these equations with our numerical data, which provides independent access to σ, p, T, and $\dot{\gamma}$ in different shearing geometries.

We first test equation (14) in simple shear flow. Our measurements permit us to determine α as a function of packing fraction as shown in figure 14 for frictionless ($\mu = 0$) and frictional ($\mu = 0.4$) cases. For frictionless granular materials α appears to be exponential in density, whereas for frictional granular materials, α does not take on an obvious functional form.

Next, we test the STZ prediction of equation (25). In figure 15 we have plotted σ/p as a function of $\dot{\gamma}/\sqrt{T}$ for frictional and non-frictional granular materials in both simple shear flow and incline flow. The line drawn through the data is a fit to equation (25). The fit matches the data from both flowing geometries very well .

To construct the fit, we have used the data from *the simple shear cell only*: this fit permits us to extrapolate the rheology for the flow down an incline plane, even at the approach of the repose angle. This shows that an accurate determination of the coefficients from the STZ equation (25) in one shearing geometry allows for prediction in a different shearing geometry.

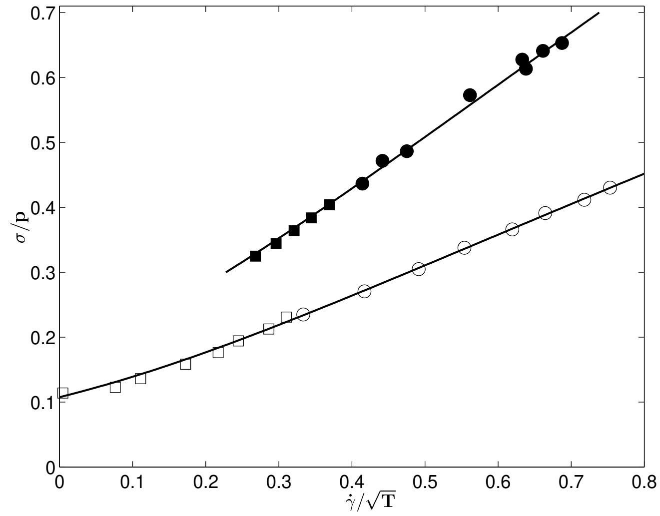

FIG. 15: σ/p plotted against $\dot{\gamma}/\sqrt{T}$ for frictional (filled symbols) and non-frictional (open symbols) granular materials. The circles correspond to data from simple shear flow and the squares to data from steady state incline flow. The line is a best fit to the steady state STZ equation 25, where only the data from the simple shear flow geometry was used to construct the best fit. This shows that STZ theory properly predicts the outcome of incline flow experiments once the parameters (which depend only on grain properties) are determined from simple shear experiments.

CONCLUSION

To conclude, we have implemented a numerical simulation of dense granular flows in order to clarify the microscopic origin of jamming and the specific assumptions needed to construct the STZ formulation of constitutive equations for dense granular flows.

Our first goal was to obtain detailed information on dense granular flows: on the relevance of kinetic terms and the locality of the constitutive relation. For this purpose, we implemented two different simulation configurations: a simple shear cell with Lees-Edwards periodic boundary conditions and SLLOD equations of motion and the flow of a granular material down a rough incline. In both configurations, we measured the components of the stress tensor, packing fraction ν, strain rate $\dot{\gamma}$ and granular temperature T.

In the Lees-Edward cell, we separated the kinetic, collisional and static contributions to the stress tensor. In dense systems, close to jamming, the kinetic and collisional terms appear to be orders of magnitude smaller than the static contributions. These observations indicate that the flow of a dense granular material is in a regime which is not collisional and does not verify the assumptions of kinetic theory, yet verifies Bagnold's scaling and the associated invariance of Newton's equations.

We have also observed the normal stress difference and shown that it vanishes in dense flows so that, in this regime, shear stress and pressure completely characterize the stress tensor. In each configuration we studied, the rheology of dense granular materials is thus entirely specified by five quantities: shear stress σ, pressure p, packing fraction ν, strain rate $\dot{\gamma}$ and granular temperature T, two of which are prescribed: ν and $\dot{\gamma}$ in the shear cell; σ and p for the flow down an incline. The rheology of the granular material requires us to specify three relations which determine the remaining unknowns. There are many equivalent ways these relations can be formulated, but we wished to formulate them in a way that emphasized the invariance of Newton's equations and the expected scaling form of constitutive equations.

We found that, as anticipated in [1], the relation between quantities $\dot{\gamma}/\sqrt{T}$ and σ/p was remarkably similar to the stress-strain rate relation in a normal elasto-plastic transition. We were surprised to observe the quality of the fit to the data of figure 15 with expression (25) without any density dependence of the parameters of the theory. We would have expected that these parameters might involve strong density dependence. This observation, however, strengthens the idea that the primary distinction of granular materials is the way energy balance is prescribed and that otherwise they behave like "normal" materials, once the variables are appropriately rescaled.

Another relation emerges naturally from the expectation that energy balance in granular materials should take the scaling form (14). The density-dependent parameter α accounts for the rate of dissipation of energy and we would expect it to be reasonably captured by collisional integrals of the type used in kinetic theory (at least for non-frictional materials). A proper derivation of energy dissipation in dense flows now appears as an accessible yet challenging issue that we wish to examine in future works.

Finally, a third relation remains to be specified. This relation can be, for example, a prescription for σ/p or $\dot{\gamma}/\sqrt{T}$ as a function of packing fraction. We observed this relation, but did not attempt to model it. Other works of ours [107**?** –109] on the relevance of free-volume dynamics in the rheology of dense materials seem to be related to this missing relation but we did not wish to elaborate in this direction in order to focus on the stress-strain rate relation which is the most immediate prediction of STZ theory.

As we see, the STZ theory correctly predicts one among three relations which are necessary for a complete description of dense granular flows. This relation suffices to account for the shape of the velocity profile down an incline. However it does not account for the overall amplitude of the velocity profile or for the uniform value of the density as a function of $\tan\theta$.

Note that we have compared here data from a Lees-Edward cell with the rheology of a flow down an inclined plane in the limit when the height of the granular material is large. The agreement between the two sets of data indicate that there is no long-range structure which governs the flow. This does not mean, of course, that no gradient or diffusive terms should ever intervene in a final form of the rheology of granular flows. In particular, we expect that a diffusive term should arise in equation 14, but in the large height limit this diffusive term disappears from the bulk rheology.

This brings us back to the observations by Pouliquen [79] of a relation $h_{\mathrm{stop}}(\theta)$ which governs jamming: these observations have led to the idea that non-local constitutive equations might be required to capture the rheology of granular materials. We expect these observations, however, to be "normal" finite size effects. In particular, it was observed in [1] that an exponentially decaying kernel in place of w in equation (18) was sufficient to account for large values of $h_{\mathrm{stop}}(\theta)$ when $\theta \to \theta^*$: the analytical form of the kernel used in this work was consistent with an exponential decay of correlation in the system, again consistent with the notion that local, structured correlations suffice to understand these effects.

Another puzzling observation by Pouliquen was that the amplitude of the velocity profile seemed to scale as $1/h_{\mathrm{stop}}(\theta)$. As we saw previously, this amplitude is governed by $\alpha(\nu)$ and a missing relation between *e.g.* σ/p and ν. We thus cannot provide an interpretation for these observations, but believe that our work provide important pointers to circumvent the problem and direct further progresses toward a complete description of dense granular flows.

[1] A. Lemaître, Phys. Rev. Lett. **89**, 064303 (2002).
[2] M. L. Falk and J. S. Langer, Phys. Rev. E **57**, 7192 (1998).
[3] M. L. Falk and J. S. Langer, M.R.S. Bulletin **25**, 40 (2000).
[4] A. Schofield and C. P. Wroth, *Critical state in soil mechanics* (Mc Graw-Hill, New York, 1968).
[5] R. L. Brown and J. C. Richard, *Principles of powder mechanics* (Pergamon, New York, 1970).
[6] K. H. Roscoe, Geotechnique **20**, 129 (1970).
[7] R. M. Nedderman, *Statics and Kinematics of Granular Materials* (Cambridge University Press, Cambridge, 1992).
[8] A. Mehta and G. C. Barker, Rep. Prog. Phys. 383 (1994).
[9] H. M. Jaeger and S. R. Nagel, Rev. Mod. Phys. **68**, 1259 (1996).
[10] Jacques Duran, *Sables, poudres et grains* (Éditions Eyrolles, Paris, 1997).
[11] P. de Gennes, Physica A **261**, 267 (1998).
[12] J. Rajchenbach, Adv. Phys. **49**, 229 (2000).
[13] L. P. Kadanoff, Rev. Mod. Phys. **71**, 435 (1999).
[14] H. Hertz, J. Reine Angew. Math. **92**, 156 (1881).
[15] K. L. Johnson, *Contact Mechanics* (Cambridge University Press, Cambridge, 1985).
[16] H. M. Jaeger and S. R. Nagel, Science **255**, 1523 (1992).
[17] H. M. Jaeger, S. R. Nagel, and R. P. Behringer, Rev. Mod. Phys. **68**, 1259 (1996).
[18] P. A. Cundall and O. D. L. Strack, Geotechnique **29**, 47 (1979).
[19] A. Drescher and Dejossel.G, J. Mech. Phys. Sol. **20**, 337 (1972).
[20] D. M. Mueth, H. M. Jaeger, and S. R. Nagel, Phys. Rev. E **57**, 3164 (1998).
[21] D. W. Howell, R. P. Behringer, and C. T. Veje, Chaos **9**, 559 (1999).
[22] D. Howell, R. P. Behringer, and C. Veje, Phys. Rev. Lett. **82**, 5241 (1999).
[23] R. A. Bagnold, Proc. Roy. Soc. London A **255**, 49 (1954).
[24] R. A. Bagnold, Proc. Roy. Soc. London A **295**, 219 (1966).
[25] M. L. Hunt, R. Zenit, C. S. Campbell, and C. E. Brennen, J. Fluid. Mech. **452**, 1 (2002).
[26] L. E. Silbert *et al.*, Phys. Rev. E **64**, 051302 (2001).
[27] c. S. O'Hern *et al.*, Phys. Rev. E **68**, 011306 (2003).
[28] L. E. Silbert, J. W. Landry, and G. S. Grest, Physics of Fluids **15**, 1 (2003).
[29] J. M. Hill and Y. H. Wu, Proc. Roy. Soc. London A **48**, 67 (1992).
[30] D. Harris, Proc. Roy. Soc. London A **450**, 37 (1995).
[31] J. M. Hill and X. M. Zheng, Acta Metall. **118**, 97 (1996).
[32] S. B. Savage, J. Fluid. Mech. **92**, 53 (1979).
[33] S. B. Savage and D. J. Jeffrey, J. Fluid. Mech. **110**, 255 (1981).
[34] J. T. Jenkins and S. B. Savage, J. Fluid. Mech. **130**, 187 (1983).
[35] C. K. K. Lun, S. B. Savage, D. J. Jeffrey, and N. Chepurniy, J. Fluid. Mech. **140**, 223 (1984).
[36] J. T. Jenkins and M. W. Richman, Physics of Fluids **28**, 3485 (1985).
[37] C. K. K. Lun and S. B. Savage, J. Appl. Mech. **54**, 47 (1987).
[38] S. B. Savage, in *Theoretical and applied mechanics*, edited by P. Germain, M. Piau, and D. Caillerie (Elsevier, Amsterdam, 1989), pp. 241–266.
[39] C. S. Campbell, Annu. Rev. Fluid Mech. **22**, 57 (1990).
[40] K. Hutter and K. R. Rajagopal, Cont. Mech. & Therm. **6**, 81 (1994).
[41] N. Sela and I. Goldhirsch, Physics of Fluids **7**, 507 (1995).
[42] N. Sela, I. Goldhirsch, and S. H. Noskowicz, Physics of Fluids **8**, (1996).
[43] N. Sela and I. Goldhirsch, J. Fluid. Mech. **361**, 41 (1998).
[44] J. W. Dufty, Advances in Complex Systems **4**, 397 (2001).
[45] P. K. Haff, J. Fluid. Mech. **134**, 401 (1983).
[46] P. K. Haff, J. Rheol. **30**, 931 (1986).
[47] M. A. Hopkins and M. Y. Louge, Physics of Fluids A. **3**, 47 (1991).
[48] I. Goldhirsch and G. Zanetti, Phys. Rev. Lett. **70**, 1619 (1993).
[49] C. S. Campbell, P. W. Cleary, and M. Hopkins, J. Geophys. Res. **100**, 8267 (1995).
[50] A. V. Potapov and C. S. Campbell, Physics of Fluids **8**, 2884 (1996).
[51] Y. Zhang and C. S. Campbell, J. Fluid. Mech. **237**, 541 (1992).

[52] C. S. Campbell, in *Powders and grains 93*, edited by C. Thornton (A. A. Balkema, Rotterdam, Netherlands, 1993), pp. 289–294.
[53] V. V. R. Natarajan, M. L. Hunt, and E. D. Taylor, J. Fluid. Mech. **304**, 1 (1995).
[54] E. Azanza, Ph.D. thesis, École Nationale des Ponts et Chausées, 1998.
[55] E. Azanza, F. Chevoir, and P. Moucheront, J. Fluid. Mech. **400**, 199 (1999).
[56] J. Choi, A. Kudrolli, R. R. Rosales, and M. Z. Bazant, Phys. Rev. Lett. **92**, (2004).
[57] K. I. Kanatani, Int. J. Eng. Sc. **17**, 419 (1979).
[58] N. Mitarai, H. Hayakawa, and H. Nakanishi, Phys. Rev. Lett. **88**, 174301 (2002).
[59] A. C. Eringen, in *Contributions to mechanics*, edited by D. Abir ("", New-York, 1969), pp. 23–40.
[60] S. B. Savage, J. Fluid. Mech. **377**, 1 (1998).
[61] W. Losert, L. Bocquet, T. C. Lubensky, and J. P. Gollub, Phys. Rev. Lett. **85**, 1428 (2000).
[62] L. Bocquet *et al.*, Phys. Rev. E **65**, (2000).
[63] L. Bocquet, J. Errami, and T. C. Lubensky, Phys. Rev. Lett. **89**, (2002).
[64] L. Bocquet *et al.*, Phys. Rev. E **65**, (2002).
[65] S. B. Savage, in *Mechanics of granular materials: new models and constitutive relations*, edited by J. T. Jenkins and M. Satake (Elsevier, Amsterdam, 1983), pp. 261–282.
[66] P. C. Johnson and R. Jackson, J. Fluid. Mech. **176**, 67 (1987).
[67] P. C. Johnson, P. Nott, and R. Jackson, J. Fluid. Mech. **210**, 501 (1990).
[68] J. T. Jenkins and E. Askari, J. Fluid. Mech. **223**, 497 (1991).
[69] K. G. Anderson and R. Jackson, J. Fluid. Mech. **41**, 145 (1992).
[70] M. Y. Louge, Phys. Rev. E **67**, (2003).
[71] I. S. Aranson, L. S. Tsimring, and V. M. Vinokur, Phys. Rev. E **60**, 1975 (1999).
[72] I. S. Aranson and L. S. Tsimring, Phys. Rev. E **6402**, (2001).
[73] D. Volfson, L. S. Tsimring, and I. S. Aranson, Phys. Rev. E **68**, 021301 (2003).
[74] P. Mills, D. Loggia, and M. Tixier, Europhysics Letters **45**, 733 (1999).
[75] O. Pouliquen and R. Gutfraind, Phys. Rev. E **53**, 552 (1996).
[76] D. Ertaş and T. C. Hasley, Europhysics Letters **60**, 931 (2002).
[77] C. S. Campbell and C. E. Brennen, J. Fluid. Mech. **151**, 167 (1985).
[78] H. J. Herrmann and S. Luding, Cont. Mech. & Therm. **10**, 189 (1998).
[79] O. Pouliquen, Physics of Fluids **11**, 542 (1999).
[80] C. S. Campbell, J. Fluid. Mech. **465**, 261 (2002).
[81] J. J. Moreau, in *Nonsmooth mechanics and application: courses and lectures*, edited by J. J. Moreau and P. D. Panagiotopoulos (Springer-Verlag, Vienna, 1988), pp. 1–82.
[82] M. Jean and J.-J. Moreau, in *Proceedings of Contact Mechanics International Symposium* (Presses Polytechniques et Universitaires Romandes, Switzerland, 1992), pp. 31–48.
[83] J. J. Moreau, in *Powders and Grains*, edited by C. Thornton (Brookfield, Rotterdam, Netherlands, 1993), pp. 227–232.
[84] J. J. Moreau, Eur. J. Mech. A-Solids **13**, 93 (1994).
[85] J. J. Moreau and M. Jean, in *Engineering systems design and analysis*, edited by A. Lagarde and M. Raous (Am. Soc. Mech. Eng., New York, 1996), pp. 201–208.
[86] A. W. Lees and S. F. Edwards, J. Phys. C **5**, 1921 (1972)
[87] D. J. Evans and G. P. Morriss, Phys. Rev. A **30**, 1528 (1984).
[88] D. J. Evans and G. P. Morriss, *"Statistical Mechanics of Nonequilibrium Liquids"* (Academic Press, London, 1990).
[89] M. Alam and S. Luding, J. Fluid. Mech. **476**, 69 (2003).
[90] I. Goldhirsch and N. Sela, Phys. Rev. E **54**, 4458 (1996).
[91] R. Larson, *The structure and rheology of complex fluids* (Oxford University Press, New York, 1999).
[92] F. Chevoir, M. Prochnow, J. Jenkins, and P. Mills (unpublished).
[93] S. Ogawa, in *US-Japan seminar on continuum mechanical and statistical approaches in the mechanics of granular materials*, edited by S. Cowin and M. Satake (Gakujutsu Bunken Fukyu-Kai, Tokyo, 1978), pp. 208–217.
[94] V. Garzó and J. W. Dufty, Phys. Rev. E **59**, 5895 (1999).
[95] M. L. Falk, Phys. Rev. B **60**, 7062 (1999).
[96] J. S. Langer, Phys. Rev. E **64**, 011504 (2001).
[97] J. S. Langer and L. Pechenik, Phys. Rev. E **68**, 061507 (2003).
[98] J. S. Langer, L. Pechenik, and M. L. Falk, Phys. Rev. E **69**, ?? (2003).
[99] K. Maeda and S. Takeuchi, Phys. Stat. Sol. A **49**, 685 (1978).
[100] K. Maeda and S. Takeuchi, J Phys-F-Metal Phys **8**, L283 (1978).
[101] K. Maeda and S. Takeuchi, Phil. Mag. A **44**, 643 (1981).
[102] D. Srolovitz, K. Maeda, and T. Egami, Phil. Mag. A **44**, 847 (1981).
[103] S. Takeuchi and K. Maeda, Key Eng. Mater. **13-15**, 749 (1987).
[104] D. Deng, A. S. Argon, and S. Yip, Phil. Trans. Roy. Soc. **329**, 549 (1989).
[105] A. Argon and H. Kuo, Mater. Sc. Eng. **39**, 101 (1979).
[106] A. Argon and L. Shi, Acta Metall. **31**, 499 (1983).
[107] A. Lemaître, Phys. Rev. Lett. **89**, 195503 (2002).
[108] A. Lemaître, A Dynamical Approach to Glassy Materials, cond-mat/0206417, 2002.
[109] A. Lemaître, "Out-of-equilibrium relaxation of a time-dependent effective temperature", cond-mat/0307216, 2002.